Equilibrium, Isotherm and Thermodynamic Studies of the Adsorption of Methylene Blue from Aqueous Solution onto Unmodified Biochar (UBC) of African Oil-bean (*Pentaclethra Macrophylla*) Seed Shell

[1]Iromaka Stanislaus Chika, [1]Njoku Victor Obinna, [1]Duru Chidi, [1]Isiuku Beniah Obinna, [2]John-Dewole Olusegun Onimisi, [1]Nwabueze Benjamin I and [1]Adindu Chinonso Blessing

[1]Department of Chemistry, Imo State University, Owerri, Nigeria
[2]Department of Chemical Sciences, Lead City University, Ibadan
*Correspondence: johndewole.olusegun@lcu.edu.ng ORCID 0000-0003-4883-7750

Abstract: The development of low-cost and recyclable adsorbents is an urgent need in the field of wastewater treatment. There has been growing research interest in exploiting agricultural waste for cost-effective removal of different pollutants including dye colour in water bodies. In this study, unmodified Biochar of African oil-bean seed shells (UBC) was prepared as adsorbent. The adsorption of methylene blue (MB) dye from aqueous solution onto UBC was studied by analyzing the effect of contact time, initial dye concentration, pH and temperature on the amount of MB dye adsorbed per unit mass of the adsorbent. An optimum adsorption capacity, q_t of 27.8 mg/g was achieved during 90 min contact time using initial dye concentration of 250 mg/L of UBC adsorbent. The adsorption of the MB dye increased with increase in the initial dye concentration, time and pH but decreased with increase in temperature. The adsorption mechanism of the dye obeyed the Freundlich isotherm model. The thermodynamic study showed that adsorption of MB onto the adsorbent was spontaneous, exothermic and had good affinity of the biosorbent toward MB. The adsorbent was characterized with Fourier transform infra-red (FTIR) spectroscopy, scanning electron microscopy (SEM) and Brunauer-Emmett-Teller (BET). The findings highlight African oil-bean seed shell biochar as a potential low-cost adsorbent for cationic dyes.

[Iromaka Stanislaus Chika, Njoku Victor Obinna, Duru Chidi, Isiuku Beniah Obinna, John-Dewole Olusegun Onimisi, Nwabueze Benjamin I and Adindu Chinonso Blessing. **Equilibrium, Isotherm and Thermodynamic Studies of the Adsorption of Methylene Blue from Aqueous Solution onto Unmodified Biochar (UBC) of African Oil-bean (*Pentaclethra Macrophylla*) Seed Shell.** *J Am Sci* 2026;22(3):36-47]. ISSN 1545-1003 (print); ISSN 2375-7264 (online). http://www.jofamericanscience.org. 04. doi:10.7537/marsjas220326.04

Keywords: Adsorbents; *Pentaclethra macrophylla;* methylene blue dye; adsorption isotherm; adsorption thermodynamics

Introduction

Concentrations of dye in aqueous solution or wastewater from textile industries have been lowered using low-cost adsorbents such as fly ash, sorbents prepared from agricultural, industrial, and biological waste materials[1,2,3]. Deficiency of clean water is a global concern. The primary cause of clean water deficiency is very much due to water pollution. Water is the most basic necessary requirement of life[4]. However, the growing industrialization has created a deep impact on human health and the environment by introducing large quantity of untreated wastewater into our surroundings[5]. Textile industry is one of the most water-consuming industries and is listed as the main contributor of water pollution due to the tremendous amount of wastewater containing dyes released to the environment[6]. More than 7 x 10^5 tonnes of dyes are produced annually by this particular industry and it was estimated by the World Bank that approximately 17 % to 20 % of the world industrial water pollution emanates from both treatment and dyeing of textiles[7].

Methylene blue (MB) is a heterocyclic aromatic compound. As a cationic (basic) dye, MB, is a water-soluble dye which was chosen as a model contaminant since it is one of the most important and widely used dyes in textile and paper industries[7]. Potential side-effects of MB dye include tissue necrosis, mental confusion, methemoglobinemia and vomiting of MB toxicity[8]. Environmental adverse effects of dyes include restriction of penetration of sunlight and oxygen transfer into aquatic organisms[8,9]. Methods applied for the removal of dyes in wastewater include; adsorption, flocculation, oxidation, electrolysis, biodegradation, ion-exchange, filtration, membrane process and ozonation[7,10].

Adsorption is a process by which solid surface concentrations or other fluids attract component(s) in a liquid to its surface and form an attachment via physical or chemical bond and thus the process removes the component(s) from the liquid. It is also the process by which atoms, ions or molecules from a gas, liquid or dissolved solid adhere to a surface[11]. Advantages of adsorption over other methods of dye

removal include; cost-effectiveness, high efficiency, simple operation conditions, and no generation of harmful by-products[8,9,10,11].

Factors affecting dye adsorption in aqueous systems include contact time (saturation time), initial dye concentration, temperature, solution pH, and adsorbent dosage (adsorbent concentration). *Pentaclethra macrophylla* Benth, the oil-bean tree, is the sole member of the genus occurring naturally in the humid lowlands of West Africa. It is a leguminous tree (family: Leguminosae; sub-family: Mimosoideae)[12]. *Pentaclethra macrophylla* has been cultivated in Nigeria since 1937[12]. Enormous amounts of African Oil-bean (*Pentaclethra macrophylla*) seed shells wastes are generated after the use of the useful parts. These wastes pose disposal challenges due to limited or no information on what they can be used for. This causes environmental menace. There has not been any known literature in which this adsorbent has been applied to adsorb MB dye. Hence, the research aims study its adsorbent potentials.

MATERIALS AND METHODS

Adsorbate Preparation

MB dye used in this work as the adsorbate is a product of Luxion, China. It was purchased from laboratory chemicals supply company in Owerri, Imo State, Nigeria and used directly without further treatment. MB is a synthetic cationic (basic) dye soluble in water. Its structure is as shown in figure 1. It has molecular formula of $C_{16}H_{18}N_3SCL.3H_2O$, molecular mass, 373.9g/mol. and wavelength of maximum absorbance (λmax), 663nm.

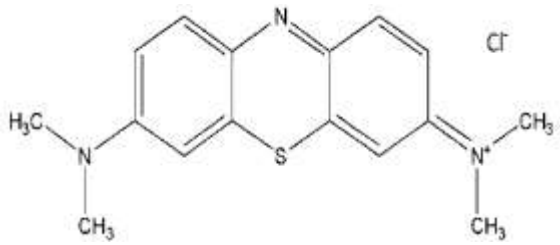

Figure 1: Structural formula of MB

The adsorbate solution was prepared by dissolving 1.0 g of MB powder in 1,000 cm^3 of solution using distilled water to obtain the stock solution of 1,000 mg/L. Working solutions of 25 to 250 mg/L were prepared from the stock by serial dilutions.

Adsorbent Preparation

African oil-bean (*Pentaclethra macrophylla*,) seeds were obtained from the tree in Obowo, Imo State, Nigeria. They were shelled and the seed shells washed four times with tap water. They were further washed three times with distilled and deionized water, sun-dried for four days and ground into small particles size using manual grinder (Corona, Landers YC1A. S.A. Table top, S.A). It was then ground further using electric grinder (Corona mills, REF 121, S.A.) and oven-dried at 105 ^{0}C for 8 hr to constant weight using the laboratory oven (LG, MC 2886, China). The ground, dried seed shells were sieved with 600 μm and 841 μm sieve size.

The prepared sample was then pyrolysed in the electric furnace at 600 ^{0}C for 2 hr at heating rate of 10 ^{0}C/min. Nitrogen gas at flow rate of 0.1 m^3/hr was used as purge gas to keep the whole process inert[12]. The biochar produced was cooled to 30 ^{0}C and stored in air-tight container after milling into powder and sieving with laboratory mesh size of 600 μm and 841 μm. This product is the unmodified biochar (UBC) of African oil-bean seed shell.

Characterization of the UBC Adsorbent

Quantachrome high speed surface area and pore size analyzer model: Nova 4200, USA were used for the textural characterization of the UBC adsorbent. Surface area and pore size/pore volume determinations on the UBC adsorbent were made using Brunauer-Emmette-Teller (BET) and Berrett-Joyner-Halenda (BJH) respectively. Agilent Technologies Microlab Cary 630 Fourier Transform Infrared (FTIR) spectrophotometer was employed to record the spectra of the UBC adsorbent in the investigation of the surface chemistry of the adsorbent. Data analysis was focused on the 400 to 4,000 cm^{-1} region. The sample was formed into pellets with potassium bromide (KBr). 1 mg of UBC was encapsulated in 100 mg of KBr for the infrared (IR) study. The adsorbent (before and after adsorption) were collected in transmission and the background corrected in each case. The shift in the adsorption band of the FTIR spectra in the adsorbent after adsorption from those of the adsorbent before adsorption gave an insight on the functional groups responsible for the adsorption of MB[13]. Scanning Electron Microscope (SEM), Phenom Prox model, was used to examine the morphology and structure of the UBC adsorbent before and after MB adsorption. The pH point of zero charge (pHpzc), the pH at which the surface of an adsorbent is neutral was determined using pH drift method[14].

Batch Adsorption Equilibrium Experiments

These experiments were carried out in 250 ml conical flasks covered with glass stoppers using 200 ml working solution of 150 mg/L and 1 g adsorbent. The flasks were agitated at constant speed of 120 rpm for 190 min in a water bath shaker (Thermofisher Scientific, SWB 15 Thermostated, USA) at 30 ^{0}C. The influence of initial dye concentration, was carried out at 25, 50, 100, 150, 200 and 250 mg/L, contact time at 10, 20, 30, 60, 90, 120, 150, 160, 170, 180, 190 and 200 mins. pH at 2, 3, 4, 5, 6, 7, 8, 9, 10, 11 and 12 and temperature at 30, 35, 40, 45 and 50 ^{0}C. Other conditions remain constant. pH was adjusted using dilute HCl and NaOH. Samples were collected at predetermined time intervals, and analysed for residual dye concentration in solution using UV vis spectrophotometer (Model Shimadzu UV 752, M/s. Shimadzu, Japan) at the wavelength of 663nm. Calculation of the amount of MB dye adsorbed per unit of adsorbent, (mg/g) and the removal percent (%) were made using equations 1, 2 and 3 respectively.

Triplicate measurements were made and the mean value used

$$q_e = \frac{(C_o - C_e)V}{m} \quad (1)$$

Where q_e (mg/g) is the amount of MB adsorbed per unit mass of adsorbent; C_o is initial MB concentration in liquid phase; C_e is liquid phase MB concentration at equilibrium. The units of C_o and C_e are mg/L. V is Volume of MB solution in litre (L); m is mass of dry adsorbent used in grammes (g).

$$q_t = \frac{(C_o - C_t)V}{m} \quad (2)$$

$$R\% = \frac{C_o - C_e}{C_o} \times \frac{100}{1} \quad (3)$$

Where q_t is amount of MB adsorbed per unit mass of adsorbent at time, t. Unit of q_t is mg/g. C_t is liquid phase MB concentration at time, t. Unit of C_t is mg/L. R% is percent removal of MB.

RESULTS AND DISCUSSION

Characterization of the unmodified biochar (UBC) of *Pentaclethra macrophylla* (PM)

Figure 2 displays FTIR spectrum of UBC before and after adsorption.

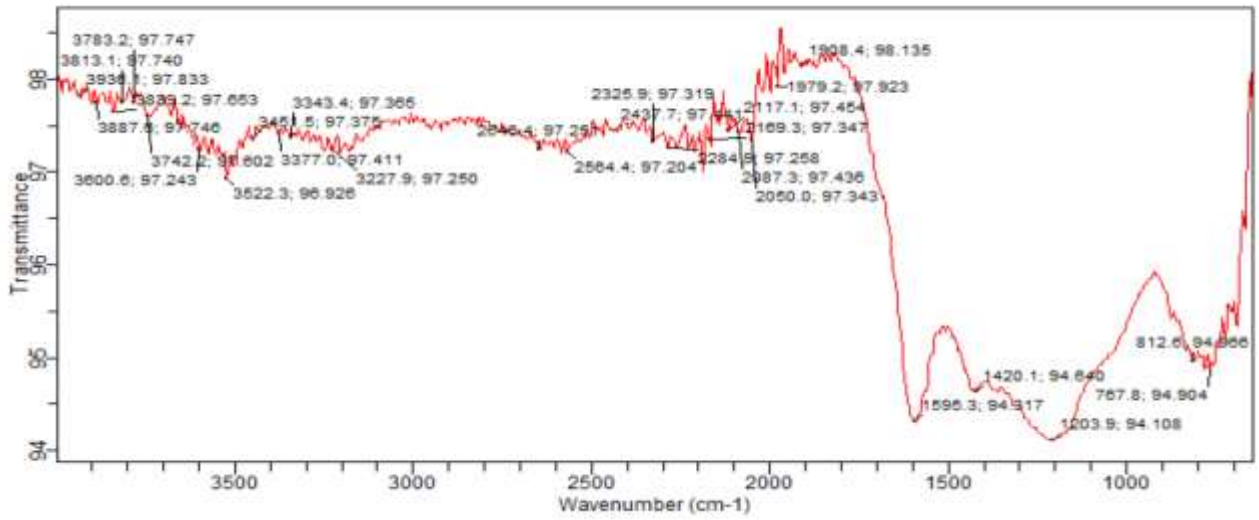

Figure 2a: Spectrum of UBC before adsorption

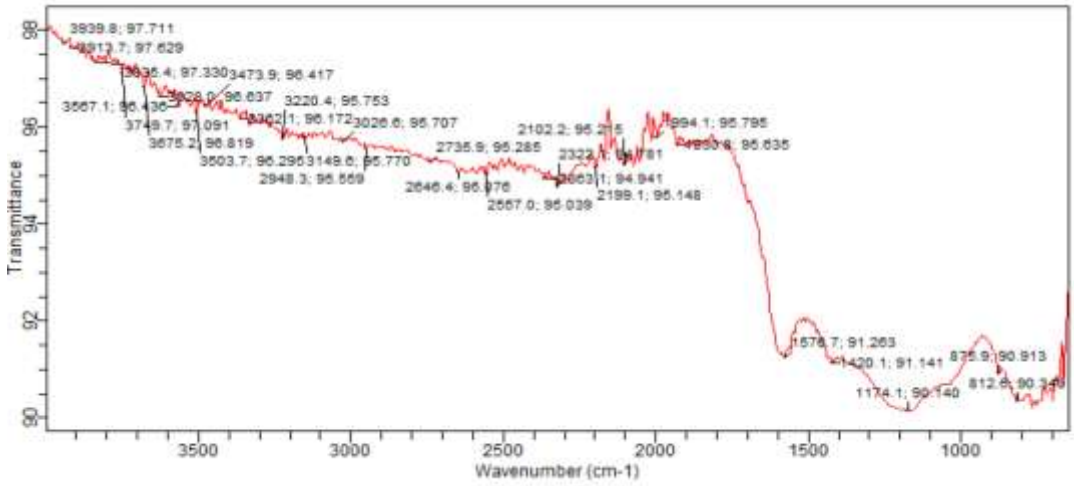

Figure 2b: Spectrum of UBC after adsorption

The strong, broad band at 3227 cm^{-1} characterizing the presence of O-H stretching vibration of carboxylic acid functional group was shifted to a band at 3220 cm^{-1} indicating O-H stretching vibration of carboxylic acid. Also shifted after adsorption was band at 2564 cm^{-1}, a broad band indicating O-H stretching vibration of carboxylic acid group. It was shifted to 2557 cm^{-1}. 1595 cm^{-1} band, 1203 cm^{-1} and 767 cm^{-1} bands all disappeared after adsorption. There were new bands at 1576 cm^{-1} and 1174 cm^{-1} after adsorption. The band at 1595 cm^{-1}, 1203 cm^{-1}, 767 cm^{-1}, 1576 cm^{-1} and 1174 cm^{-1} are ascribed respectively to N-H bending vibration of amide group, C-O stretching vibration of alcohol group, C-Cl stretching vibration of alkyl halide group, ring C=C stretching vibration of aromatic compounds and C-O stretching vibration of alcohol functional group. The functional groups of shifted and removed peaks were involved in adsorption while the retained ones were not used during adsorption.

Scanning Electron Microscopy (SEM)

SEM results before and after adsorption were presented in figure 3(a) and 3(b).

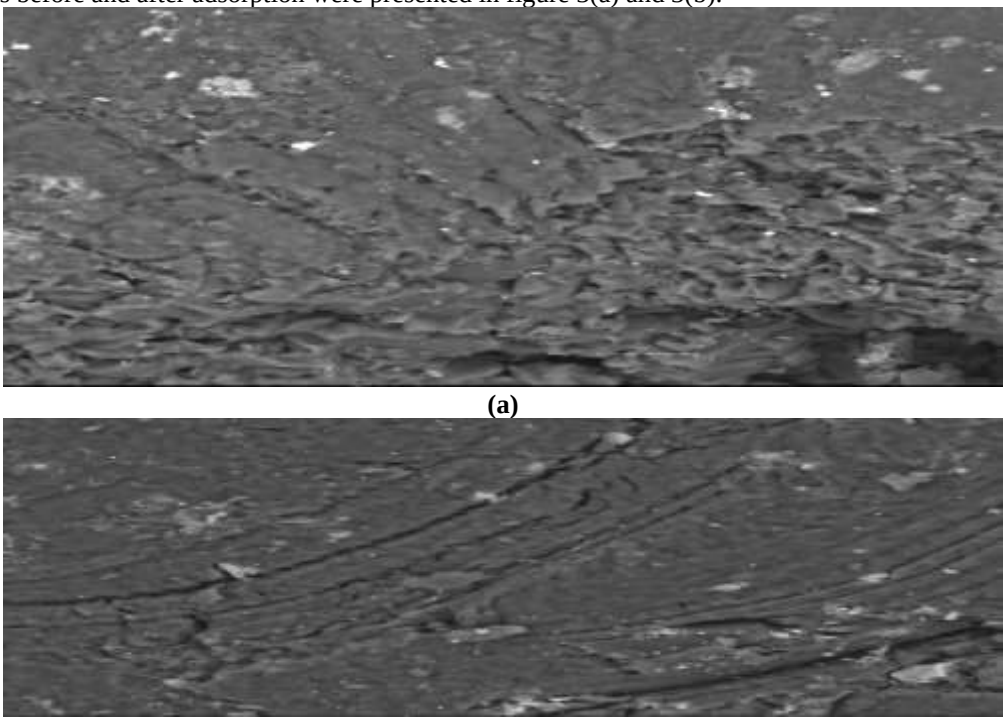

(a)

(b)

Figure 3: SEM micrographs of UBC (a) before (b) after adsorption

Numerous pores of various sizes and shapes were revealed by the SEM micrograph before adsorption which got much reduced in the image obtained after adsorption. This indicated that adsorption had taken place[15]. This showed that the UBC is a potential adsorbent.

BET and BJH Analysis

Table 1 depicts the results of BET and BJH analysis, which examined the surface area, pore volume and pore diameter of the adsorbent.

Table 1: Results of BET and BJH on UBC

Characterization of Adsorbent	Values obtained
Surface area (m^2/g)	325.5
Pore volume (cc/g)	0.132
Pore diameter (nm)	2.128

BET analysis showed surface area of the sample and the BJH, the pore volume and pore diameter of the adsorbent. The specifications of sample porosity diameter as provided by IUPAC are as follows: micropores < 2 nm, mesopores 2-50 nm, macropores > 50 nm[16]. Porous materials can act as suitable adsorbents for various fluids due to their conductive properties[17,18]. The UBC adsorbent used in this research is a mesoporous material (2.128 nm) and thus, a potential adsorbent.

Point of Zero Charge of the Adsorbent

pHpzc graph of UBC, which is the graph of ΔpH (pH_f-pH_i) against pH_i is shown in figure 4.

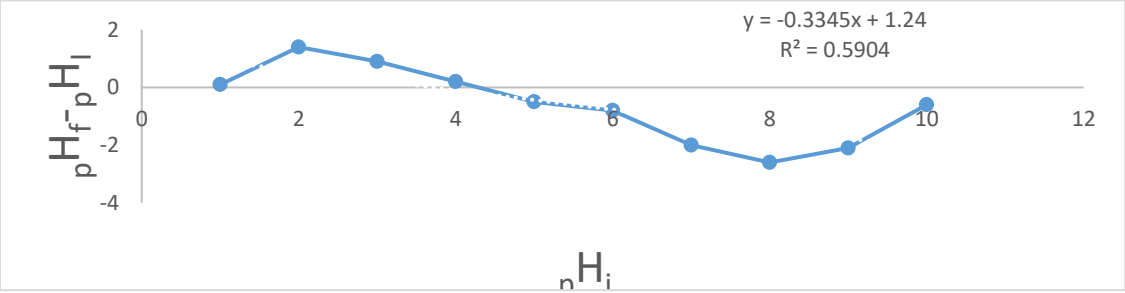

Figure 4: Graph of pHpzc for UBC

From the graph of the pHpzc, pH point of zero charge of the UBC surface lies at about pH 7.4.

Effect of Initial Dye Concentration (C_o) and Contact Time on the Adsorption

The influence of initial dye concentration and contact time in equilibrium uptake of MB from aqueous solution onto UBC is depicted in figure 5.

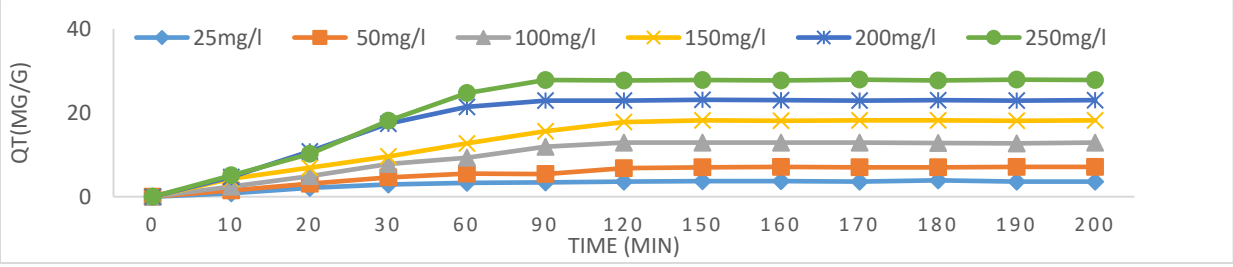

(a)

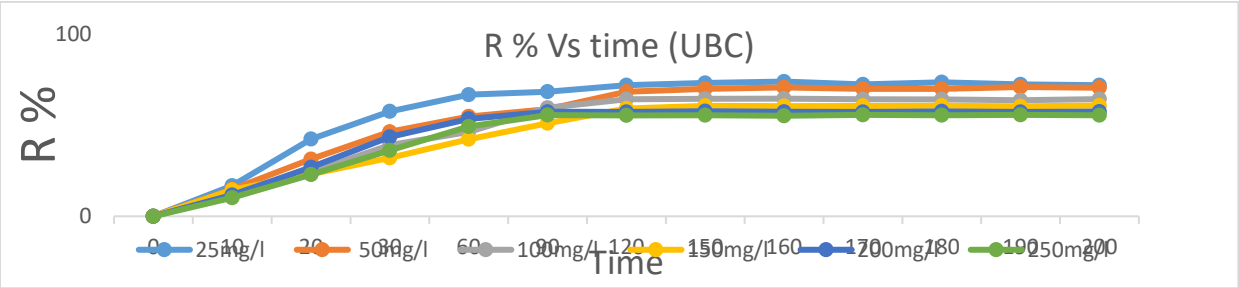

(b)

Figure 5: Effect of Initial Concentration and Time Adsorption

Figure 5(a) shows increase in adsorption capacity, q_t with time and indicating fast adsorption occurring in the early stage of adsorption because the active sites available were in abundance. This could have been caused by physical adsorption or ion exchange at the surface of adsorption[18]. Equilibrium adsorption capacities were 3.6, 7.0, 12.9, 18.2, 23.1 and 27.8 mg/g for the initial MB concentrations of 25, 50, 100, 150, 200 and 250 mg/L respectively. The rate of adsorption was then gradually reduced until saturation was attained. At the slower stage, the number of active sites became decreased and adsorption efficiency slowed down because as soon as saturation set in, additional adsorption became almost impossible. Figure 5(b) showed that as initial dye concentration (C_o) increased from 25 to 250 mg/L, R % decreased from 72.4 to 55.5 %, depicting inverse relationship. This result is in line with the trend obtained by other researchers [18,19,20]. The removal percent, R % of the adsorption of MB by UBC recorded highest value of 72.4 % at a contact time of 120 mins for initial dye concentration of 25 mg/L. Higher yields obtained in the adsorption at lower dye concentrations is as a result of interaction of most of the MB dye molecules present in the solution with the binding sites on the surface of the adsorbent. All adsorbents have limited number of binding sites which attain saturation at given concentrations[21]. Increasing amount of the MB molecules, as a result, were not adsorbed when the initial concentration of MB was progressively increased, leading to decrease in R %. At lower concentrations, most of the dye molecules in solution interacted with the active sites of the adsorbent thereby facilitating adsorption. With higher dye concentration, after saturation of the adsorbent surface, unadsorbed dye molecules keep increasing, constituting decreasing removal percent (efficiency) as observed in figure 5b.

The effect of initial dye concentration with respect to adsorption capacity on the adsorption of MB dye in aqueous solution onto UBC is presented in figure 5a. As C_o increased from 25 to 250 mg/L, equilibrium adsorption capacity increased from 3.6 to 27.8 mg/g respectively. Adsorption capacity, q_t increased with increase in initial MB concentration due to increasing concentration gradient[22]. The increasing concentration gradient acted as increasing driving force. This force acted to overcome all mass transfer resistances of the MB molecules between the aqueous and solid phase as initial MB concentration increased. This lead to continued increase in adsorption capacity until saturation of the adsorbent active sites was attained[23,24,25].

Effect of pH on the adsorption of MB from aqueous solution onto UBC:

Solution pH is quite closely related to adsorption efficiency. This is because change in pH can cause adsorbent surface charge to be affected by protonation or deprotonation[26]. It also affects the degree of adsorbate ionization and speciation[27]. The effects of the different pH environments on adsorption capacity, q_e and MB removal percent, R % are depicted in figure 6(a) and 6(b) respectively.

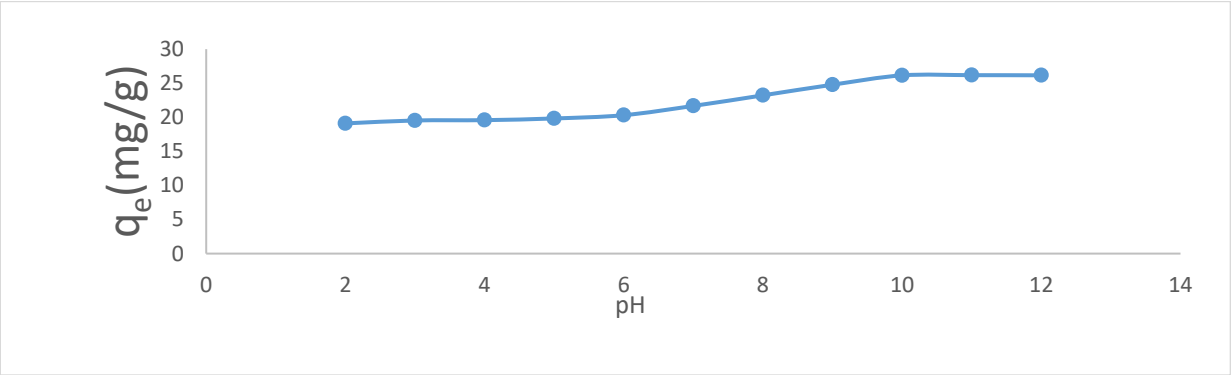

(a)

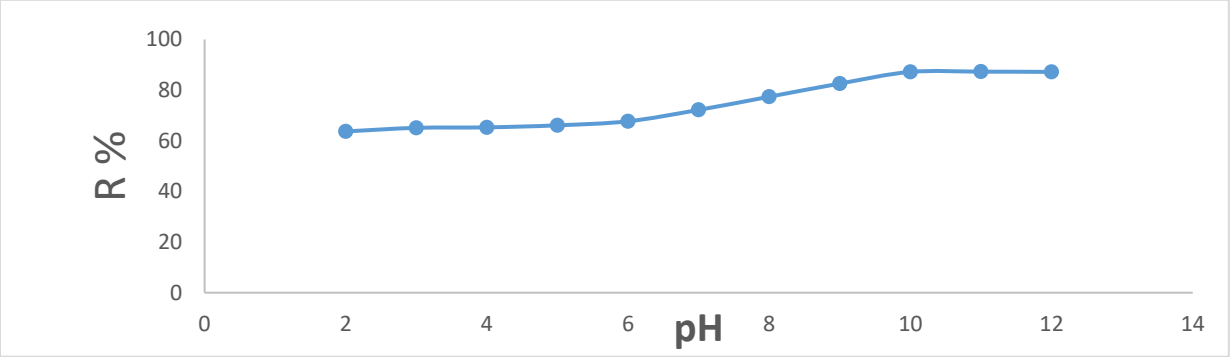

(b)

Figure 6: Graph of Effect of pH on Adsorption

Adsorption capacity, q_e and removal percent, R % increased with increase in solution pH as seen in figure 6 (a) and (b). q_e and R % values increased slowly at low pH (acidic). At these pH values there was electrostatic repulsion between the H^+ ions of the solution on the UBC surfaces and the positive ions of the MB dye (MB dye being a cationic dye). It is observed from the figures that after pH 6.3, sharp increases in q_e and R % values were recorded. These sharp rise in q_e and R % occurred after pH value exceeded the pHpzc of UBC (pH 6.3). There was competition between the H^+ ions at lower pH and the cation groups of the MB dye for adsorption sites. As the solution pH increased there came a decrease in the H^+ charge density. Hence the electrostatic repulsion between the cationic MB dye and the MB surface became reduced. This resulted to increase in the rate of adsorption[28]. Solution pH influenced the kinetics of the adsorption. For the cationic dye, as pH increased, the proton concentration decreased. This enhanced the chances of more dye molecules to react with the active sites on the adsorbent surface due to reduced proton competition[29].

Effect of Temperature

Temperature has significant impact on adsorption process. The effect of temperature was investigated at five different temperatures (30, 35, 40, 45 and 50 ^{0}C). The results are displayed in figures 7(a) and 7(b). It was seen from the figures that temperature had an inverse relationship with adsorption capacity, q_e and removal percent, R %. As temperature was raised from 30 to 50 ^{0}C, q_e and R % decreased from 18.17 to 16.32 mg/g and 60.6 to 54.4 % respectively. Maximum q_e and R % were at 30 ^{0}C for both. The decrease in q_e and R % as temperature increased is likely to be as a result of desorption. The increase in available thermal energy may be the cause of the desorption. Higher temperature induces higher mobility of the adsorbate molecules. Beyond certain temperature, it results to desorption. Conversely, decrease in temperature resulted to adsorption increase meaning that the process of adsorption was exothermic[30].\

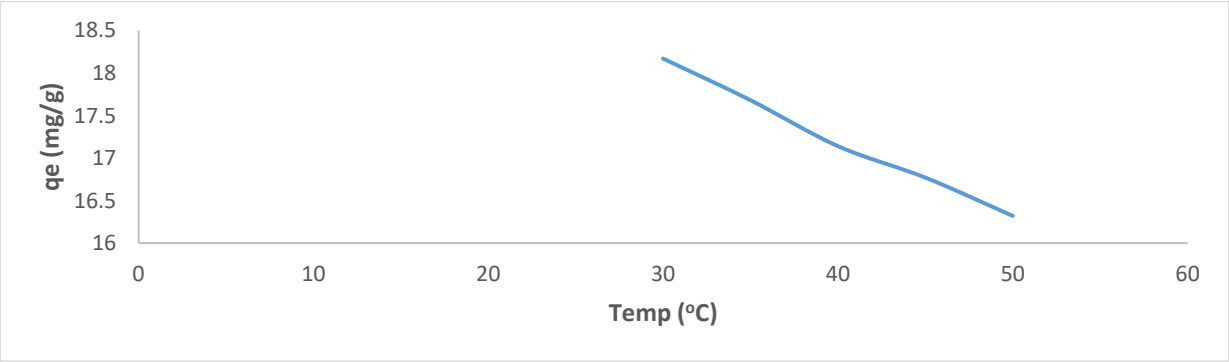

(a)

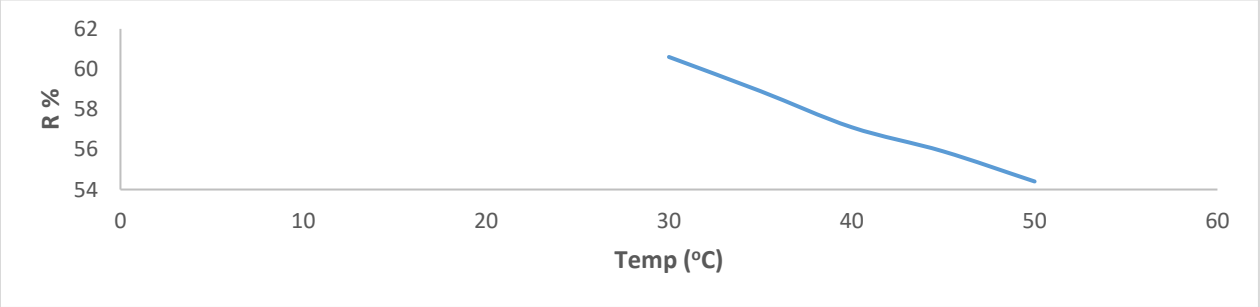

(b)

Figure 7: Effect of Temperature on the Adsorption

Adsorption Isotherm

The plot that describes the way equilibrium concentration of adsorbent varies with the concentration of liquid phase at given temperature and pH is known as adsorption Isotherm. Such diagrammatic models are used to illustrate the interaction of adsorbent with the adsorbate under equilibrium condition at constant temperature[31].

Freundlich Isotherm Model

Assumes the occurrence of multilayer adsorption on heterogeneous surfaces of adsorbent. It also assumes that active sites with higher energy are occupied first. With increase in the amount of adsorbate deposited on each other on the active sites, number of layers increase and binding forces decrease exponentially[32,33].

Freundlich isotherm model in its linearized form is presented in equation (6)

$$\log q_e = \log K_F + \frac{1}{n}\log C_e \quad (6)$$

Where K_F and n are freundlich isotherm constants related to adsorption capacity and adsorption intensity respectively. q_e and C_e are as explained for Langmuir isotherm model. The value of n gives the favourability of adsorption.

The closer $^1/_n$ is to zero, the more heterogeneous the adsorbent surface becomes. $^1/_n$ value of 0.2 to 0.8 (good adsorption); 1/n values of 0.2 and below (better adsorption and stronger bond between adsorbate particles and adsorbent adsorption sites)[34].

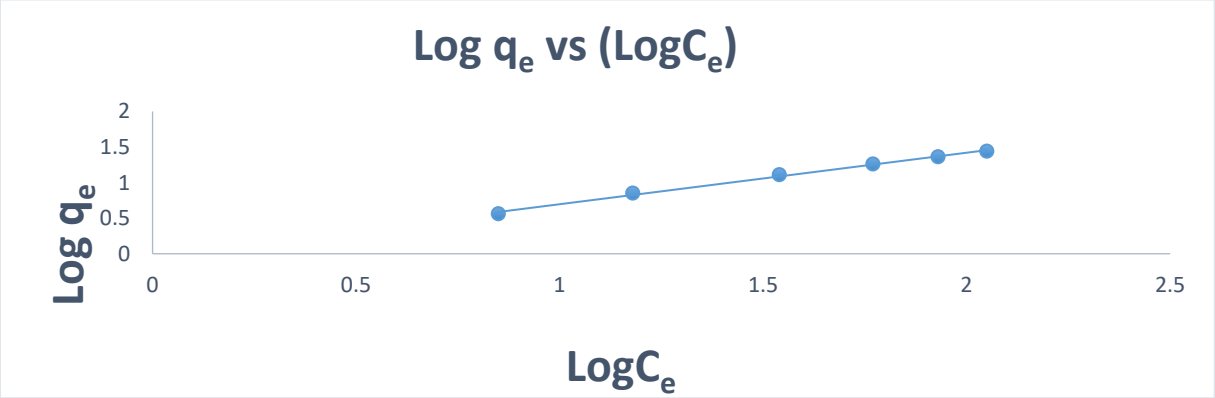

Figure 8: Freundlich Isotherm for UBC

Freundlich adsorption isotherm model recorded the highest linear regression correlation coefficient, R^2 of 0.9960 (very close to unity) indicating that Freundlich isotherm model was the most fitted model for this adsorption process. This suggests that the adsorption of MB onto UBC involved multi-layer adsorption with interactions between the MB molecules. It implied that the surface of the UBC was heterogeneous.

Adsorption Thermodynamics

Figure 9: Van't Hoff plot for UBC

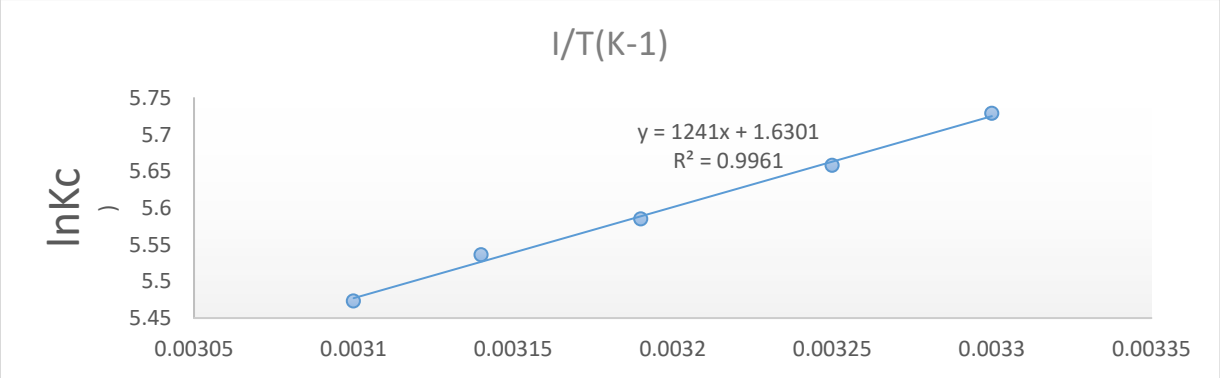

Positive ΔH^0 value indicated endothermic adsorption process while negative value showed that the process was exothermic. The ΔH^0 was – 10.318 kJ/mol showing exothermic adsorption process.
+13.552J/mol ΔS^0 value obtained as shown in the table implied increased randomness at the solid/solution interface during the adsorption process[35]. All the values of ΔG^0 obtained in this work were negative (-14.70 to -14.43 kJ/mol) showing spontaneous process at all temperatures investigated. These negative values of ΔG^0 also implied that the adsorptions of MB at these temperatures do not need to be promoted by external forces. It was also observed from the table that the value of ΔG^0 decreased with increase in temperature implying that the heat application benefitted the adsorption process[36]. Values of ΔG^0 from -20 to KJ/mol indicate physisorption while values less than -40 kJ/mol imply chemisorption[36]. It was therefore concluded that the adsorption of MB from aqueous solution onto UBC was of physical nature.

Conclusion

Biochar was prepared with *Pentaclethra macrophylla* (African oil-bean) seed shell at a temperature of 600 ^{0}C using nitrogen purge system to make the system of preparation inert. FTIR was used to characterize the biochar (UBC) before and after adsorption which revealed functional groups present such as carboxylic acid group, alcohol group, alkyne and amide groups which were identified as taking part in the adsorption process. SEM image of the adsorbent showed large number of pores of various sizes suggesting UBC as a potential adsorbent. BET and BJH calculations and analysis showed high surface area and pore sizes revealing that the adsorbent was a porous material suitable for adsorption.

Examination of the effects of initial dye concentration on the adsorption showed that the adsorption capacity increased with initial dye concentration and with time until saturation while percent removal decreased with increase in initial dye concentration but increased with time. Rapid increase of adsorption capacity, q_e occurred after the pHpzc of the adsorbent was exceeded. An optimum pH of 10 was recorded at a maximum q_e of 26.15 mg/g. The maximum q_{t-} (adsorption capacity at given time, t of 90 minutes) was 27.8 mg/g. q_e decreased with increase in temperature (30 ^{0}C to 50 ^{0}C).
Freundlich isotherm model best explained the process; showing physical, heterogeneous adsorption with multilayer formation. Langmuir (Monolayer) maximum adsorption capacity, q_m was 49.5 mg/g. The adsorption was exothermic, of increasing randomness and spontaneous. From the results of this investigation, UBC showed potential of a promising adsorbent.

Declaration of Competing Interest:
The authors declare that they have no conflict(s) of interest. All authors have read, understood, and have complied asapplicable with the statement on "Ethical Responsibilities of Authors" as found in the Instructions for Authors in this journal.

Correspondence to:
Olusegun Onimisi, John-Dewole
Department of Chemical Sciences
Lead City University, Ibadan
Email: johndewole.olusegun@lcu.edu.ng
ORCiD 0000-0003-4883-7750

References

1. Njoku, V.O. And Hameed, B.H.: Preparation and Characterization of Activated Carbon from Corncob by Chemical Activation with H_3PO_4 for Dictorophenoxyacetic Acid Adsorption. *Chem. Eng. J.*, 173: (2011) 391-399.
2. Dolui D, Das A, Hasanuzzaman M, Adak MK. Physiological and biomolecular interventions in the bio-decolorization of Methylene blue dye by Salvinia molesta D. Mitch. International Journal of Phytoremediation. 2025 Jan 28;27(2):215-32.
3. Bayram O, Özkan U, Kardeş S, Moral E, Göde F, Pehlivan E. Sustainable decolorization of methyl blue and malachite green from an aqueous environment using magnetic biochar prepared from the fruit seeds of Mespilus germanica L. Chemistry and Ecology. 2025 Apr 21;41(4):528-51.
4. Ugendar CM, Pani AS, Rambabu K, Naina, Singh P, Sivakumar K, Rahaman M, Bahadur I, Prasad C. A TD-DFT Exploration and Artocarpus heterophyllus Plant Leaf Extract-Based Decolorization of Methylene Blue. Water, Air, & Soil Pollution. 2026 Feb;237(3):147.
5. Marefatyan F, Salimi F, Ghobadifard M, Mohebbi S. The impressive photoactivity of Ag/CeCoO 3 for methylene blue dye decolorization under illumination. Reaction Chemistry & Engineering. 2025;10(11):2683-95.
6. Putra AM, Amirta R, Suwinarti W, Alisha GD, Haqiqi MT. Effective decolorization of methylene blue by Nypa fruticans husk: Screening and optimization. InIOP Conference Series: Earth and Environmental Science 2025 Dec 1 (Vol. 1562, No. 1, p. 012031). IOP Publishing.
7. Karimian S, Shariat M, Mashayekhi H. Deep insight into methyl blue decolorization using non-thermal pulsed plasma: experimental and modeling approaches. Scientific Reports. 2025 Sep 26;15(1):32989.
8. Thabet M, El-Monaem EM, Mouhafid M, Abdel-Lateef MA, Seaf-Elnasr TA, Alruwaili YM, Alanazi AH, Ali HM, Mohamed A, Cheira MF, Gomaa H. A Hybrid Mesoporous Sulphur-doped CoMn Oxide@ Cobalt Alginate-derived Carbon Spongy-like Beads for Methylene Blue Decolorization: Isotherm, Kinetic, and Machine Learning Modeling. Environmental Processes. 2025 Jun;12(2):16.
9. Mohanavel B, Kesavan K, Jyothi NS, Shalini R. Nickel and strontium-doped zinc oxide: A promising sorbent for methyl orange and methylene blue decolorization. Journal of Physics and Chemistry of Solids. 2025 Jul 1;202:112694.
10. Alghamdi, W.M. And El Mannoubi, I: Investigation of Seeds and Peels of *Citrullus Colocynthis* as Efficient Natural Adsorbent for MB Dye. *Processes* 9: (2021)1279

11. Alhawtali, S., El-Harbawi, M., Al-Awadi, A.S, El Blidi, L., Alrashed, M.M. And Yin, C.Y. Enhanced Adsorption of MB using Phosphoric Acid-Activated Hydrothermal Carbon Microphoreses Synthesized from A Variety of Palm-Based Biowastes. *Coatings* 13, (2023) 1287.

12. Al-Mahmoud, S.M. Kinetic and Thermodynamic Studies for the Efficient Removal of MB using *Hordeum Murinum* as A New Biosorbent. *Egypt J. Chem.* 63(9): (2020) 3381-3390.

13. Aydin, M.I., Ozaktac, D., Yuzer, B., Dogu, M., Inan, H., Okten, H. E., Coskun, S. and Selcuk, H.: Desalination and Detoxification of Textile Wastewater by Novel Photocatalytic Electrolysis Membrane Reactot for Ecosafe Hydroponic Farming. *Membr.* 12(1): (2022) 10.

14. Basha, K., El-Monaem, A., Eman, M., Khalifa, R.E., Omer, A.M. and Eltaweil, A.S. Sulfonated Grapheme Oxide Impregnated Cellulose Acetate Floated Beads for Adsorption of MB Dye: Optimization Using Response Surface Methodology. *Sci. Rep.* 12: (2022) 1-17

15. Bokil, S.A., Topare, N.S. and Khedkar, S.V. Batch Adsorption Studies on Treatment of Textile Industry Effluent Using Bamboo and Green Coconut Shell Activated Carbon. *IOP Conf. Ser:Mater Sci. Eng.* 983(1):012005 (2020) .

16. Bu, Z., Fang, Y.,Chen, H., Zhang, M. and Wang, F. Study on the Adsorption Properties of Organically Modified Diatomite for MB. Sci. Rep. 15: (2025)27561.

17. Cseri, L., Topuz, F., Abdulhamid, M.A., Alammar, A., Budd, P.M. and Szekely, G. Electrspun Adsorptive Nanofibrous Membranes from Ion Exchange Polymers to Snare Textile Dyes from Wastewater. *Adv. Mater. Technol.* 6(10): (2021) 2000955.

18. Duru, C.E., Duru, I.A., Ogbonna, C.E., Enedoh, M.C. and Emele, P. Adsorption of Copper Ions from Aqueous Solution onto Natural and Pretreated Maize Husk: Adsorption Efficiency and Kinetic Studies. *J. Chem Soc. Nigeria*, 44(5): (2019a) 798 -803.

19. Duru, C.E., Nnabuchi, M.A. and Duru, I.A. Adsorption of Cu onto Maize Husk Lignocelluloses in Single and Binary Cu-Zn Solution Systems: Equilibrium, Isotherm, Kinetic, Thermodynamic and Mechanistic Studies, *Egypt. J. Chem*., 62(7) 2019b 1695-1705.

20. Eltaweil, A.S., Abd El-Monaem, E.M., El-Subruiti, G.M., Ali, B.M., Abd El-Latif, M.M. And Omer, A.M. Graphene Oxide Incorporated Cellulose Acetate Beads for Efficient Removal of MB Dye: Isotherms, Kinetic, Mechanism and Co-Existing Ions Studies. J. Porous Mater. 30, (2023) 607-618

21. Georgin, J., Franco, D.S.P., Netto,M.S., Allasia, D., Oliveira, M.L.S. And Dotto, G.L. Treatment of Water Containing MB by Biosorption Using Brazilian Berry Seeds (*Eugenia Uniflora*). *Environ. Sci. Pollut. Res.* 27: (2020) 20831-20843

22. Goudjil, S., Guergazi, S., Masmoudi, T. and Achour, S. Effect of Reactional Parameters on The Elimination of Congo Red by the Combination of Coagulation- Flocculation with Aluminum Sulfate. Desalin Water Treat. 209: (2021) 429-436.

23. Han, Z., Wang, K., Zhang, Y., Xian, A., Wei, X. and Wang Z. Study on Methyleme Blue Adsorption Properties of Biochar/Montmorillonite Composites. *Earth Sci.* 13(4): (2024) 163-181.

24. Haowen L., Xiaohan, W., Ximg, L., Yi, s., Shicheng, Z., Qianshi, S., Zhaofan, T., Experimental Studies on N-Heptane Prolytic Characteristics in CO_2/H_2O Atmosphere. *J. Anal. And Appl. Pyrolysis*, 154: (2021) 104999

25. Hurairah, S.N., Lajis, N.M. And Halim, A.A. MB Removal from Aqueous Solution by Adsorption on *Archidendron Jiringa* Seed Shells. J. Geosci. Environ. Prot., 8: (2020) 128-143.

26. Isiuku, B.O., Paul, C.O. And Chibuike, D.E. Batch Adsorption Isotherm Models Applied in Single and Multicomponent Adsorption Systems – A Review. *J. Dispersion Sci. And Techno.*, Doi:10.1080/01932691.2021.1964988.

27. Jawad, A.H., Saber, S.E.M., Abdulhameed, A.S., Reghioua, A. Alothman Z.A. And Wilson, L.D. Mesopourous Activated Carbon from Mangosteen (*Garcinia Mangostana*) Peels by H_3PO_4 Assisted Microwave: Optimization, Characterization and Adsorption Mechanism for MB Dye Removal. *Diam. Relat. Mater*., 129: (2022) Article 109389

28. Kavci, E., Erkmen,J. And Bingol, M.S. Removal of MB Dye from Aqueous Solution using Citric Acid Modified Apricot Stone. Chem. Eng. Commun. 210: (2023) 165-180.

29. Kuang, Y., Zhang, X. And Zhou, S. Adsorption of MB in Water onto Activated Carbon by Surfactant Modification. *Water* (Switzerland) 12(2): (2020) 1-19.

30. Kumari, S., Verma, A., Sharma, P., Agarwal, S.,Rajput, V.D., Minkina, T., Rajput, P., Singh, S.P. And Garg, M.C. Introducing Machine Learning Model to Response Surface Methodology for Biosorption of MB dye Using *Triticum Aestivum* Biomass. *Sci. Rep.* 13(1): (2023) 8574.

31. Marszalek, J. And Zylla, R. Recovery of Water from Textile Dyeing using Membrane Filtration Processes. *Process.* 9(10): (2021) 1833.

32. Olugbenga, S.B., Temitope, C.A., Oluwakemi, C.A. And Abimbola, M.O. Sequestering A Nonsteroidal Anti-Inflammatory Drug Using Modified Orange Peels. *Applied Water Science*, 10: (2020) 172.

33. Olugbenga, S., Bello, Oluwol, A. Olusegun1., And Njoku, V.O. "Flash Ash: An Alternative to Powdered Activated Carbon for The Removal of Eosin Dye from Aqueous Solutions". *Bull. Chem. Soc.* Ethiop. 27(2): (2013) 191-204.

34. Patil, C.S., Kadam, A.N., Gunjal, D.B., Naik, V.M., Lee, S.W., Kolekar, G.B. And Gore A.H. Sugarcane Molasses Derived Carbon Sheet and Sea Sand Composite for Direct Removal of MB from Textile Wastewater: Industrial Wastewater Remediation Through Sustainable, Greener and Scalable Methodology. *Sep. Purif. Technol* 247: (2020) 116997.

35. Ramesh, K., Gnanamangai, B.M. And Mohanraj, R. Investigating Techno-Economic Feasibility of Biologically Pretreated Textile Wastewater Treatment by Electrochemical Oxidation Processes Towards Sludge Concept. *In J. Environ. Chem. Eng.* 9(5): (2021) 106289.

36. Senem, Y. And Merilyn, M. Agricultural Low-Cost Waste Adsorption of MB and Modeling Linear Isotherm Method Versus Nonlinear Prediction. *Clean Techn. Environ. Policy (Springer)*. (2024)